ARTICLE IN PRESS

Materials Today: Proceedings xxx (xxxx) xxx

Contents lists available at ScienceDirect

Materials Today: Proceedings

journal homepage: www.elsevier.com/locate/matpr

Ecofriendly synthesis of pure and modified $CuMnO_3$: It's application as gas sensor

Ganesh Dabhade [a,*], Gaurav Daware [b,*], Yennam Rajesh [b], Lakshmana Rao Jeeru [c], Shilpa Sangle [d], Yogita Shelke [d], Ashok V. Borhade [d]

[a] Department of Applied Science, K. K. Wagh I. E. E. and R. Nasik (MS), 422003, India[1]
[b] Department of Chemical Engineering, K. K. Wagh I. E. E. and R. Nasik (MS), 422003, India[1]
[c] School of Petroleum Technology, Pandit Deendayal Petroleum University, Gujarat 382426, India
[d] Department of Chemistry, HPT Arts and RYK Science College Nasik, India[1]

ARTICLE INFO

Article history:
Available online xxxx

Keywords:
Mixed metal oxide
Mechanochemical
Hydrothermal route
Gas sensor

ABSTRACT

Recently, novel materials like gas-sensing metal oxides, mixed metal oxides, and modified mixed metal oxides have attracted great attention owing to their key roles in monitoring environmental pollution, security in hospitals, homes, and public places, and hazardous emissions from industries and automobile exhaust. Initially, the mechanochemical (MCh) method was employed for the synthesis of the $CuMnO_3$ catalyst and then the modification of $CuMnO_3$ through the hydrothermal route. These synthesized catalysts were characterized by Ultraviolet Violet-Diffused Reflectance (UV-DRS) spectroscopy, Fourier Transform Infrared Spectroscopy (FTIR), and Scanning Electron Microscopy (SEM). The average particle size obtained for 3 % Fe/$CuMnO_3$ was found to be 14–28 nm. The present work proclaimed that among all the synthesized 1,3,5 % Fe/$CuMnO_3$ materials, the 3 % Fe modified $CuMnO_3$ material shows significant gas sensing properties towards highly toxic H_2S gas released from sewage plants, oil, and natural gas industries, among NH_3, CO_2, H_2S, H_2, CO_2 and Cl_2 with moderate temperature requirements and excellent selectivity.

Selection and peer-review under responsibility of the scientific committee of the Advances in Water Treatment and Management (ICAWTM-22).

1. Introduction

In the last few decades, perovskite as a mixed metal oxide has attracted wide attention owing to its several interesting properties like superconductivity, insulator, ion conductor, dielectricity, and ferroelectricity [1]. Perovskite also has promising significance in different areas like microelectronic circuit fabrication, sensors, piezoelectric devices, fuel cells, lasers, magnets, and efficient catalysts [2–7]. For the synthesis of perovskite-type mixed metal oxide (MMO) [8–10], numerous methods are used, all of which are laborious, difficult, and time-consuming, so we used the simple, cost-effective MCh method. The literature survey exhibits the metal-Mn-O system shows diversified significance as an effective catalyst in a wide area owning to its shape, size, and crystalline structure [11–15]. Furthermore, careful inspection of the literature specifies time-consuming that the Cu-Mn-O system of MMO has very remarkable significance in environmental cleaning owing to its potential candidature for several catalytic reactions [16,17]. Hence, author chose the most efficient and environmentally suitable Cu-Mn-O system in the current study.

Recently, gas sensing metal oxides, mixed metal oxides, and modified mixed metal oxides have gained great attraction owing to their key role in monitoring environmental pollution carbon credit, security in hospitals, homes, and public places, and hazardous emissions from industries, and automobile exhaust. A literature survey reveals that metal oxides were used as gas sensing materials to detect fatal poisonous gases such as Cl_2, CO, H_2S, H_2, NH_3, CO_2, etc., but a high-temperature requirement with low sensitivity was noticed [18–22]. Hydrogen sulphide (H_2S) is a highly toxic and inflammable gas released from sewage plants, oil, and natural gas industries. Different chemical industries and research laboratories require large amounts of H_2S gas. The occupational

* Corresponding authors.
E-mail addresses: gbdabhade81@gmail.com (G. Dabhade), gbdaware@kkwagh.edu.in (G. Daware).
[1] Affiliated to S. P. Pune University.

https://doi.org/10.1016/j.matpr.2022.08.453
2214-7853/
Selection and peer-review under responsibility of the scientific committee of the Advances in Water Treatment and Management (ICAWTM-22).

"exposure limit" is 20–100 ppb. The gas sensitivity of In_2O_3 thick film at 250 °C was reported by Xu et al. [23].

It includes preparation, analysis, and gas sensing application of $CuMnO_3$ and a 3 % Fe/$CuMnO_3$ catalyst. Initially, the synthesis of the $CuMnO_3$ catalyst (MCh method) was followed by the modification of $CuMnO_3$ by the hydrothermal route. This synthesized catalyst was characterized by different instrumental techniques like UV-DRS, FTIR, and SEM. Among all synthesized pure and modified $CuMnO_3$; 3 % Fe/$CuMnO_3$; MMO shows significant gas sensing properties towards highly toxic gas such as H_2S gas among the NH_3, CO_2, H_2S, H_2, CO, and Cl with moderate temperature requirement with better sensitivity and excellent selectivity.

2. 2.Materials and methodology

2.1. Materials and methods

Pure CuO and MnO_2 (99.99 percent purity, Sigma-Aldrich) are significantly used for the synthesis of MMO, and $CuMnO_3$ without any purification. All the chemicals are used at analytical grade. The TMAX-KFB1100 is a CE-certified muffle furnace (maximum temperature range of 1000 °C to 1100 °C) effectively used for calcination purposes. The Shimadzu IR-Affinity in the range of 4000–500 cm^{-1} was used to record the different vibrational modes, and the surface morphology of the catalyst was obtained by SEM-JSM-6300 (JEOL).

2.2. Synthesis of a catalyst

In the above-mentioned method, an A.R. grade equimolar (1:1) amount of CuO (Lancaster) and MnO_2 (Merck) were mixed thoroughly, and the removal of some water-soluble impurities was conducted by washing the powder with distilled water and drying at 110 °C. The dried precursors were subjected to stepwise calcination (after every 3 h, the sample was removed from the furnace and ground) by heating to terminal temperature. The muffle furnace was programmed at a rate of 10 °C per minute. After heating at 180 °C for 3 h, the material was cooled and milled with an agate mortar and pestle to obtain a fine crystalline powder. The obtained product was further subjected to calcination at 900 °C for the next 20 h followed by grinding and milling in hot conditions. A polycrystalline black-colored powder of $CuMnO_3$ (98 % yield) was analyzed by the above-mentioned different analytical techniques [24,25].

3. Result and discussion

3.1. Characterization of $CuMnO_3$ and 3 % Fe/$CuMnO_3$

The vibrational frequency below 700 cm^{-1} shown by the infrared spectrum confirms (Fig. 1-a) that the Cu-O-Mn bond formation and the peaks between 910 cm^{-1} and 1200 cm^{-1} are due to the stretching mode of vibration of new Fe-O-Mn (Fig. 1-b) confirms the formation of the $CuMnO_3$ and Fe modified $CuMnO_3$. SEM image attribute the surface morphology of $CuMnO_3$ and Fe modified $CuMnO_3$ with uneven surface area shows excellent catalytic activity and is depicted in Fig. 2. The average particle size of 14–26 nm was estimated by using the Debye–Scherrer equation [26,27].

3.2. Thick film preparation of pure and modified $CuMnO_3$

The MCh synthesized pure $CuMnO_3$ was ground for 1.5 h to get a fine powder. Then the nanocrystalline $CuMnO_3$; MMO was mixed with separately ground ethyl cellulose (3:1 ratio of inorganic and organic), and the mixture was again thoroughly mixed and milled for 1 h. Then 2 to 3 drops of organic binder (a mixture of terpinol, butyl cellulose, and butyl sorbitol) were added in mixture –1 to get a a thixotropic paste.The glass substrate was screen printed using this paste [28,29].

Films were kept under IR for drying purposes, and then they were fired at 400 °C for 45 min, which allowed cooling naturally and gas inspection by using a steady state gas sensing system (Fig. 3).

3.3. Selectivity of $CuMnO_3$ and 3 % Fe/ $CuMnO_3$ thick film for various gases

The sensitivity of $CuMnO_3$ and 3 % Fe/$CuMnO_3$ doped $CuMnO_3$ thick film for the various gases selected for study is NH_3, CO_2, H_2S, Cl_2, CO, and H_2, and the operating temperature range of 50–400 °C for $CuMnO_3$ fired at 400 °C.

Among the various gases examined, the maximum response was observed to H_2S gas (100 ppm) with an operating temperature of 200 °C (Fig. 4-a) for $CuMnO_3$ thick film. A careful inspection of Fig. 4-a shows that the $CuMnO_3$ thick film sensor has the potential to detect various gases at dissimilar temperatures with good selectivity. This study reveals that, by using an appropriate temperature, one can apply the sensor for definite gas detection.

Similar observations are made by using a 3 % Fe/$CuMnO_3$ thick film gas sensor for dissimilar operating temperatures (50–400 °C). Fig. 4-b shows the change in gas response of H_2S (100 ppm) with an operating temperature of 200 °C. Fig. 4 (a and b) show that the response goes on increasing with operating temperature and reaches its highest at 200 °C for H_2S gas. In comparison, $CuMnO_3$ fired at 400 °C shows a sensitivity of 63 at 200 °C but 3 % Fe/$CuMnO_3$ shows 78 at 200 °C for H_2S gas. A firm conclusion can be drawn from this study that modified $CuMnO_3$ (3 % Fe/$CuMnO_3$) was observed to be more sensitive to H_2S gas than $CuMnO_3$. The adsorbed oxygen species (O_2^-, O^-, O^{2-}) on the surface of the sensors $CuMnO_3$ and 3 % Fe/$CuMnO_3$ increases with temperature, and it reaches its highest and then lowers with a further increase in operating temperature (50–400 °C).

The reason is that when a reducing gas (H_2S) comes into contact with the sensor surface, it gets oxidized. As more and more oxygen gets adsorbed on the surface of the sensor, the oxidation rate also increases, and it also depends on the nature of the gas to be detected. Hence, more electrons are released when oxidation is higher, and therefore excellent gas response.

3.4. Optimisation of operating and firing temperature

Various experiments were carried out to examine the sensitivity of $CuMnO_3$ and 3 % Fe/$CuMnO_3$ with operating temperature in order to examine the effect of the annealing temperature. In comparison, the H_2S sensing behaviour of $CuMnO_3$ and 3 % Fe/$CuMnO_3$ thick films at various temperatures was also examined under similar experimental conditions. During the design of the gas sensor, the annealing temperature plays an important role [30,31].

The crystallinity and structure evaluations were obtained by annealing the sensing material at various temperatures. The fine crystalline material is obtained to attain the expected electronic properties for applications of the gas sensor. The dependence of the sensitivity of $CuMnO_3$ and 3 % Fe/$CuMnO_3$ to 100 ppm of H_2S at annealing temperature 200–450 °C was studied. Fig. 5 (a and b) depicts variation in response to H_2S gas (100 ppm) of the $CuMnO_3$ and 3 % $CuMnO_3$ thick film. The sensitivity of both the materials was noticed to be highest when the annealing temperature was 400 °C. The annealing temperature produces more oxygen vacancies, which is responsible for enhancing the gas sensitivity.

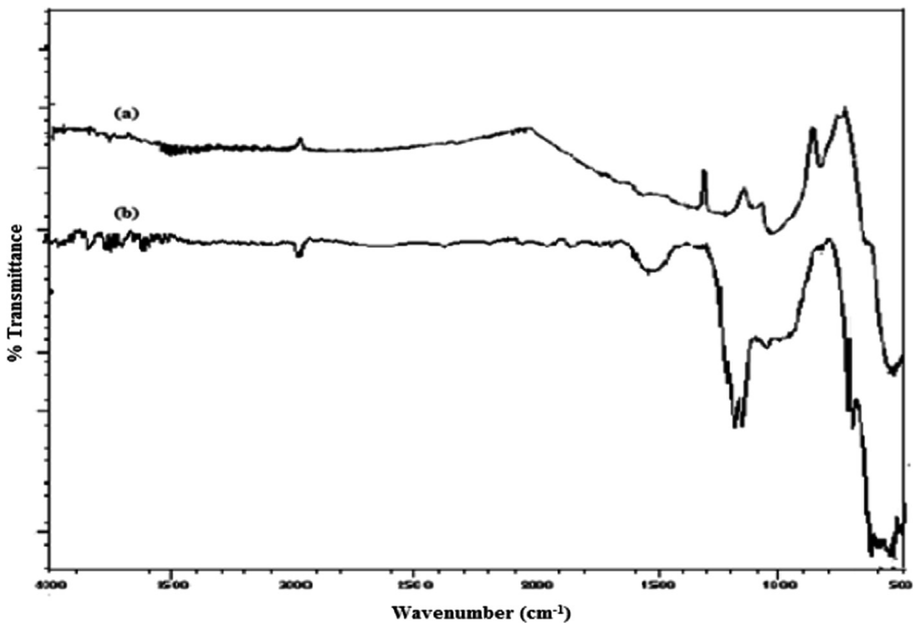

Fig. 1. FTIR spectrum of (a) $CuMnO_3$;(b) 3 % Fe/ $CuMnO_3$ catalyst.

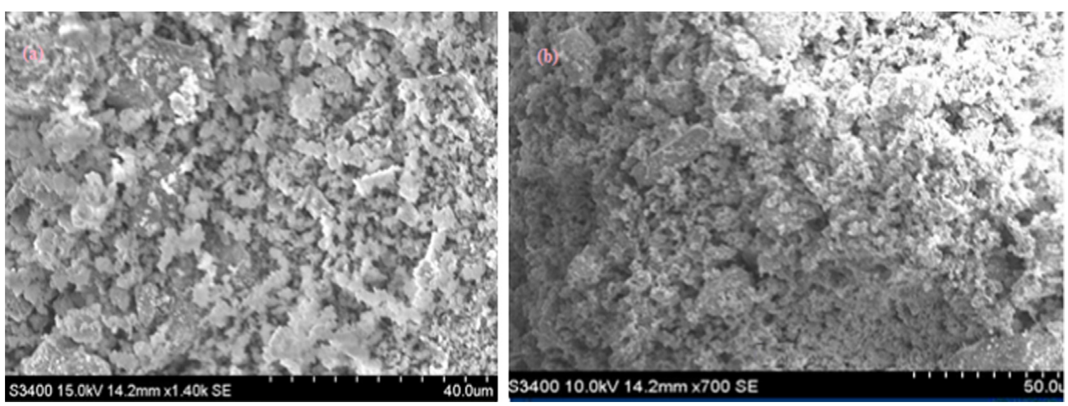

Fig. 2. SEM image (a and b) of $CuMnO_3$ and 3 % Fe/$CuMnO_3$.

Fig. 3. Photograph of steady gas sensing system.

The annealing temperature is responsible for obtaining high crystallinity in both the sensors and is probably responsible for improving the sensing properties of these thick films. Fig. 5 (a and b) show that the sensitivity of both thick films increases from 50 to 200 °C and then decreases with an increase in operating temperature. It is noticed that the highest sensitivity is 62 for $CuMnO_3$ and 79 for 3 % Fe/$CuMnO_3$ at 400 °C annealing temperature with 200 °C as an operating temperature for the H_2S gas to 100 ppm.

3.5. Sensitivity change with H_2S gas concentration

The sensitivity of $CuMnO_3$ and 3 % Fe/$CuMnO_3$ as a function of H_2S gas concentration at an operating temperature of 200 °C is depicted in Fig. 6. It is found that the sensitivity of both the synthesized materials increases from 50 to 100 ppm and shows a further decrease in sensitivity with an increase in H_2S gas concentration. At low concentrations of gas, there exists an appropriate number of sensing sites on the thick films to act upon the H_2S gas. The lower gas concentration shows less surface available for gas molecules and hence less surface reaction between adsorbed oxygen entities and H_2S gas molecules. An operating temperature of 200 °C for 100 ppm of H_2S shows maximum sensitivity. Both thick films show detection limits of 50 ppm H_2S with considerable sensitivity at an operating temperature of 200 °C. The overall conclusion

(a)

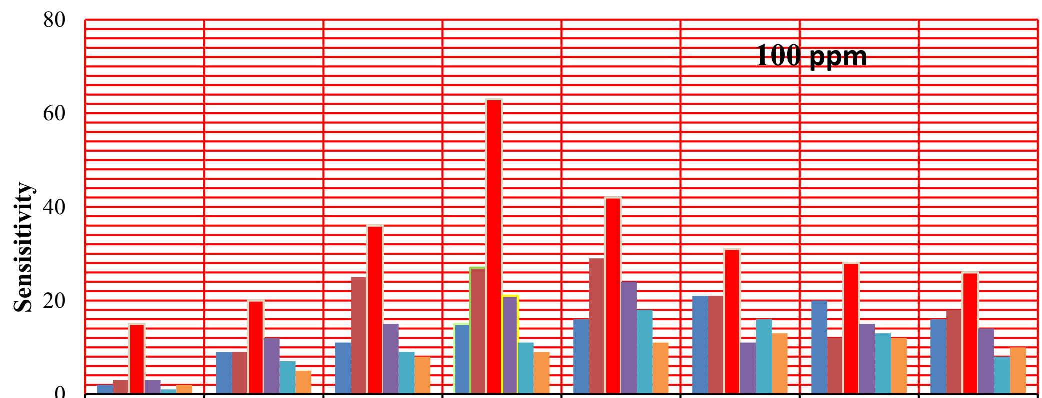

	50	100	150	200	250	300	350	400
NH3	2	9	11	15	16	21	20	16
CO2	3	9	25	27	29	21	12	18
H2S	15	20	36	63	42	31	28	26
H2	3	12	15	21	24	11	15	14
CO	1	7	9	11	18	16	13	8
Cl2	2	5	8	9	11	13	12	10

Operating Temperature ºC

(b)

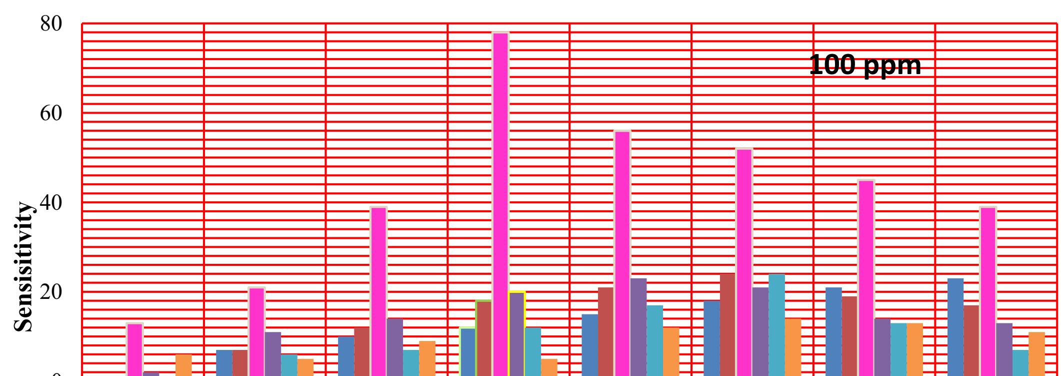

	50	100	150	200	250	300	350	400
NH3	1	7	10	12	15	18	21	23
CO2	1	7	12	18	21	24	19	17
H2S	13	21	39	78	56	52	45	39
H2	2	11	14	20	23	21	14	13
CO	1	6	7	12	17	24	13	7
Cl2	6	5	9	5	12	14	13	11

Operating Temperature ºC

Fig. 4. Sensitivity of various gases at different operating temperature for (a)$CuMnO_3$ and (b) 3 % Fe/$CuMnO_3$.

shows that 3 % Fe/$CuMnO_3$ is a superior sensor with a sensitivity of 81 to that of $CuMnO_3$ sensitivity at an operating temperature of 200 °C with 100 ppm H_2S.

3.6. Response and recovery of the $CuMnO_3$ and 3 %Fe/$CuMnO_3$ sensor

Fig. 7. depicts the response and recovery time of the $CuMnO_3$ and 3 % Fe/$CuMnO_3$ at the 100 ppm concentration of fatal H_2S gas. The H_2S gas response time and recovery time are very short, 12 *sec* and 20 *sec* for $CuMnO_3$, while 5 *sec* and 18 *sec* for 3 % Fe/$CuMnO_3$ (Fig. 7), respectively. The very quick response may be attributed to the numerous pores present on the gas sensor $CuMnO_3$, which enhances the adsorption of oxygen ions on the surface of the $CuMnO_3$, which facilitates the oxidation process of H_2S gas. In the case of the 3 % Fe/$CuMnO_3$, the response and recovery are owing to the increase in surface area of doped Fe, which ultimately increases the adsorption of gas.

4. Conclusions

In the present work, $CuMnO_3$ catalysts were successfully prepared by the MCh method and its modification by using different

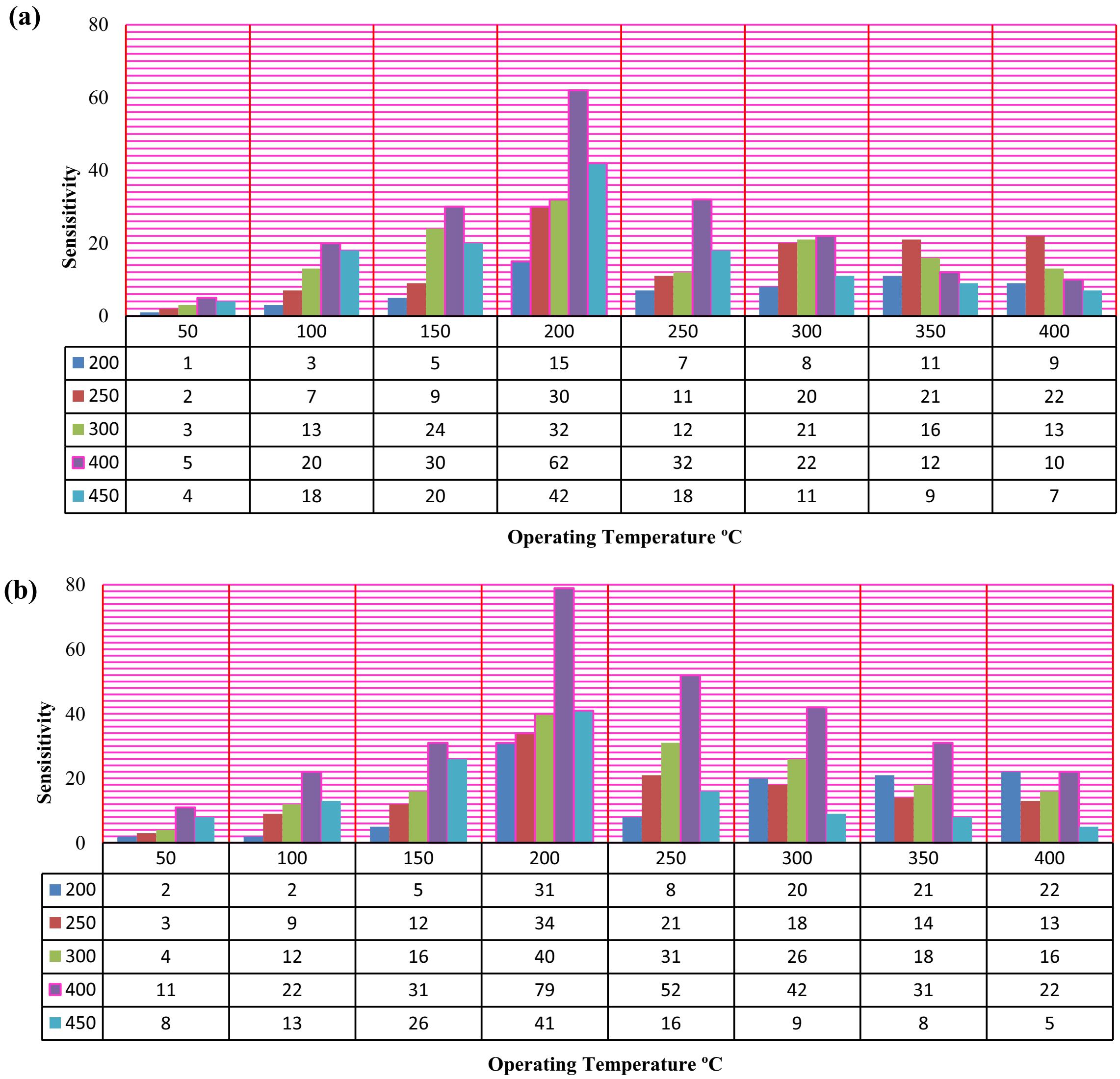

(a)

	50	100	150	200	250	300	350	400
200	1	3	5	15	7	8	11	9
250	2	7	9	30	11	20	21	22
300	3	13	24	32	12	21	16	13
400	5	20	30	62	32	22	12	10
450	4	18	20	42	18	11	9	7

(b)

	50	100	150	200	250	300	350	400
200	2	2	5	31	8	20	21	22
250	3	9	12	34	21	18	14	13
300	4	12	16	40	31	26	18	16
400	11	22	31	79	52	42	31	22
450	8	13	26	41	16	9	8	5

Fig. 5. Sensitivity of H_2S at various operating temperature against different annealed temperature.

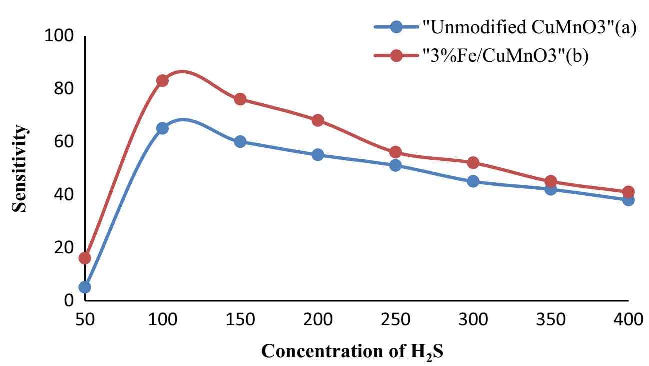

Fig. 6. Sensitivity of $CuMnO_3$ (a) and 3 %Fe/$CuMnO_3$ (b) against H_2S concentration.

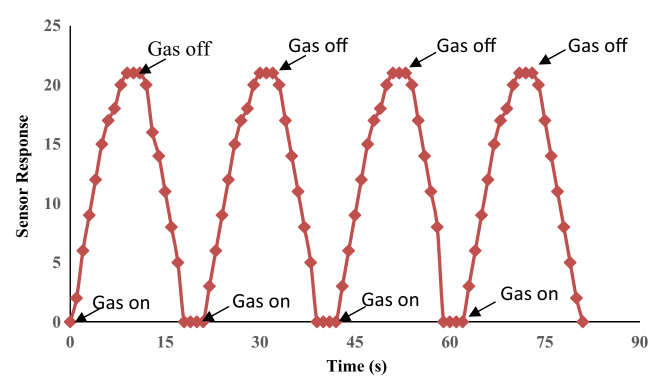

Fig. 7. H_2S response and recovery for 3 % Fe/$CuMnO_3$ gas sensor.

percent compositions of Fe through the hydrothermal route in basic media. Synthesis and phase along with plane and particle size of $CuMnO_3$ confirmed by different analytical techniques such as UV-DRS, SEM and TEM. 3 % Fe/$CuMnO_3$ is proclaimed as a favourable MMO material for the very proper detection of the fatal H_2S among various gases. In addition, the modified $CuMnO_3$ shows better sensitivity with a high response to H_2S gas than other gases at 150 °C. The 3 % Fe/$CuMnO_3$ gas sensor achieved good accuracy with better stability even for 100 ppm H_2S. The 3 % Fe/$CuMnO_3$ may facilitate response towards H_2S, which is assignable due to the drastic lattice distortion with high surface activity, which enhances the very strong interaction between surface active sites and H_2S gas.

CRediT authorship contribution statement

Ganesh Dabhade: Investigation, Methodology, Writing – original draft. **Gaurav Daware:** Conceptualization. **Yennam Rajesh:** Visualization. **Lakshmana Rao Jeeru:** Validation. **Shilpa Sangle:** . **Yogita Shelke:** Methodology. **Ashok Borhade:** Supervision.

Data availability

No data was used for the research described in the article.

Declaration of Competing Interest

The authors declare the following financial interests/personal relationships which may be considered as potential competing interests: Gaurav Daware reports administrative support, article publishing charges, equipment, drugs, or supplies, statistical analysis, travel, and writing assistance were provided by KK Wagh Institute of Engineering Education and Research.

Acknowledgements

The authors are thankful to the Management and Dr. K. N. Nandurkar, Principal of K. K. Wagh Institute of Engineering Education and Research, Nashik (Affiliated to Savitribai Phule Pune University) for providing the laboratory and infrastructural facilities and support.

References

[1] T. Mori, K. Aoki, N. Kamegashira, T. Shishido, Crystal structure of $DyMnO_3$, Mater. Lett. 42 (2000) 387–389.

[2] M.H. Sousa, F. Atourinho, J. Depeyrot, G.J. da Silva, M.C. Lara, New electric double-layered magnetic fluids based on copper, nickel, and zinc ferrite nanostructures, J. Phys. Chem. B 105 (2001) 1168–1175.

[3] K. Raj, R. Moskowitz, R. Casciari, Advances in ferrofluid technology, J. Magn. Magn. Mater. 149 (1995) 174.

[4] T. Hyeon, Y. Chung, J. Park, S.S. Lee, Y.W. Kim, B.H. Park, Synthesis of highly crystalline and monodisperse cobalt ferrite nanocrystals, J. Phys. Chem. B 6 (2002) 6831.

[5] G.R. Dube, V.S. Darshane, X-ray, electrical and catalytic studies of the system $CoFe_2O_4$–Co_2TiO_4, Bull. Chem. Soc. Jpn. 64 (1991) 2449.

[6] M.H. Kryder, Ultra high-density recording technologies, Mater. Res. Soc. Bull 21 (1996) 17–22.

[7] D.G. Mitchell, MR imaging contrast agents–what's in a name?, J Magn Reson. Imaging 7 (1997) 1–4.

[8] J. Giri, T. Sriharsha, D. Bhadur, Optimization of parameters for the synthesis of nano-sized $Co1-xZnxFe_2O_4$, $(0 \leq x \leq 0.8)$ by microwave refluxing, J. Mater. Chem. 14 (875) (2004).

[9] M. George, A.M. John, S.S. Nair, P.A. Joy, M.R. Anantharaman, Finite Size effects on the structural and magnetic properties of sol-gel synthesized $NiFe_2O_4$ powders, J. Magn. Magn. Mater. 302 (2006) 190–195.

[10] J. Wang, Prepare highly crystalline $NiFe_2O_4$ nanoparticles with improved magnetic properties, Mater. Sci. Eng., B 127 (2006) 81–84.

[11] R. Sondena, S. Stolen, P. Ravindran, T. Grande, N.L. Allan, Corner- versus face-sharing octahedra in $AMnO_3$ perovskites (A=Ca, Sr, and Ba), Phys. Rev. B 75 (2007) 184105.

[12] F.F. Fava, P.D. Arco, R. Orlando, R. Dovesi, A quantum mechanical investigation of the electronic and magnetic properties of $CaMnO_3$ perovskite, J. Phys. Cond. Matt. 9 (1997) 489–498.

[13] R. Sondena, S. Stolen, P. Ravindran, T. Grande, M. Handfland, Electronic structure and magnetic properties of cubic and hexagonal SrMnO3, Phys. Rev. B 74 (2006) 144102.

[14] J. Wang, Y.G. Su, X.Q. Wang, J.H. Chen, Z. Zhao, M.Q. Shn, The effect of partial substitution of Co in $LaMnO_3$ synthesized by sol–gel methods for NO oxidation, Catal. Comm. 25 (2012) 106.

[15] J. Chen, M. Shen, X. Wang, J. Wang, Y. Su, Z. Zhao, Catalytic performance of NO oxidation over $LaMeO_3$ (Me = Mn, Fe, Co) perovskite prepared by the sol–gel method, Catal. Comm. 37 (2013) 105–108.

[16] M.R. Morales, B.P. Barbero, L.E. Cadus, Evaluation and characterization of Mn-Cu mixed oxide catalysts for ethanol total oxidation: influence of copper content, Fuel 87 (2008) 1177–1186.

[17] M. Zimowska, Z.A. Michalik, M.T. Janik, J. Gurgul, R.P. Socha, J. Podobinski, E.M. Serwicka, Catalytic combustion of toluene over mixed Cu–Mn oxides Author links open overlay panel, Catal. Today 119 (2007) 321–326.

[18] M.S. Shinde, D.R. Patil, R.S. Patil, Ammonia gas sensing property of nanocrystalline Cu_2S thin films, Indian J. Pure Appl. Phys. 51 (2013) 713–716.

[19] Z. Chen, K. Colbow, MgO-doped Cr_2O_3: solubility limit and the effect of doping on the resistivity and ethanol sensitivity, Sens. Actuators B 9 (1992) 49–53.

[20] L.A. Patil, D.R. Patil, Heterocontact type CuO-modified SnO_2 sensor for the detection of a ppm level H_2S gas at room temperature, Sens. Actuators B 120 (2006) 316–323.

[21] D.R. Patil, L.A. Patil, P.P. Patil, Cr_2O_3-activated ZnO thick film resistors for ammonia gas sensing operable at room temperature, Sens. Actuators B 126 (368) (2007).

[22] S.A. Patil, L.A. Patil, D.R. Patil, G.H. Jain, M.S. Wagh, CuO-modified tintitanate thick film resistors as H_2-gas sensors, Sens. Actuators B 123 (2007) 233.

[23] J. Xu, J. Wang, J. Shen, Hydrothermal synthesis of In2O3 for detecting H_2S in air, *Sens. Actuators* B 115 (2006) 642–646.

[24] A.V. Borhade, D.R. Tope, G.D. Gare, G.B. Dabhade, One pot four-component synthesis of novel substituted 2-phenyl-4(3H) quinazolinones using recyclable nanocrystalline $CuMnO_3$ catalyst, J. Korean ChemSoc. 61 (2017) 157–162.

[25] A.V. Borhade, D.R. Tope, G.B. Dabhade, Removal of erioglaucine dye from aqueous medium using ecofriendly synthesized $ZnMnO_3$ photocatalyst, J. Surf. Sci. Nanotech. 15 (2017) 74–80.

[26] A.L. Patterson, The Scherrer formula for X-ray particle size determination, Phys. Rev. 56 (1939) 978.

[27] A. Monshi, M.R. Foroughi, M.R. Monshi, Modified Scherrer equation to estimate more accurately nano-crystallite size using XRD, World J. Nano Sci. Engg. 2 (2012) 154–160.

[28] G.H. Jain, V.B. Gaikwad, D.D. Kajale, R.M. Chaudhari, R.L. Patil, N.K. Pawar, M.K. Deore, S.D. Shinde, L.A. Patil, Gas sensing performance of pure and modified BST thick film resistor, Sens. Transducers 90 (2008) 160–173.

[29] K.D. Schierbaum, U.K. Kirner, J.F. Geiger, W. Gopel, Schottky-barrier and conductivity gas sensors based upon Pd/SnO_2 and Pt/TiO_2, Sens. Actuators 4 (1991) 87–94.

[30] D. Kotsikau, M. Ivanovskaya, D. Orlik, F. Falasconi, Gas-sensitive properties of thin and thick film sensors based on Fe_2O_3–SnO_2 nanocomposites, Sens. Actuators B Chem. 101 (2004) 199–206.

[31] Y. Hu, O.K. Tana, J.S. Pan, H. Huang, W. Cao, The effects of annealing temperature on the sensing properties of low temperature nanosized $SrTiO_3$ oxygen gas sensor, Sens. Actuators B 108 (2005) 244–249.